A novel detector with graphitic electrodes in CVD diamond

Alexander Oh, Benoît Caylar, Michal Pomorski, Thorsten Wengler

A novel detector with graphitic electrodes in CVD diamond

Alexander Oh a,□, Benoit Caylar b , Michal Pomorski b , Thorsten Wengler

[a] School of Physics and Astronomy, University of Manchester, Oxford Road, M13 9PL Manchester, UK

[b] CEA, LIST, Diamond Sensors Laboratory, CE Saclay, 91191 Gif-sur-Yvette CEDEX, France

[c] CERN, 1211 Geneva 23, Switzerland

Abstract

A synthetic single crystal diamond sample has been prepared with graphitic in bulk electrodes by laser induced graphitisation of diamond. A geometry with an array of electrodes has been fabricated to demonstrate the functionality of a "3D diamond detector" for ionising radiation. The detection capability has been studied with synchrotron radiation.

Keywords

Graphitic-electrodes ; 3D-detector ; Synchrotron-radiation

1. Introduction

Synthetic diamond produced via chemical vapour deposition (CVD) is an established sensor material for particle detection and has found many applications, e.g. in accelerator based experiments, synchrotrons and dosimetry applications. The radiation resistance of diamond [1] is a key property, and it is being used and proposed for detector applications [2] in harsh radiation environments.

In this letter the realisation of a novel electrode geometry is presented where the electrodes are reaching into the bulk of the detector material. The aim is to fabricate an array of graphitic micro-channels (GMCs) to apply an electric field in the bulk of the diamond, as opposed to the conventional planar electrode geometry used so far. This concept has been proven to increase the radiation resistance of silicon detectors [3] and should also be applicable to CVD diamond. The charge is collected laterally and therefore the grain boundaries present in polycrystalline material are expected to attenuate the signal [4], while for single crystal diamond this limitation is not present.

In this work graphitic electrodes have been fabricated in bulk diamond by graphitisation with a laser. Single crystal CVD diamond has been processed to create an array of GMCs. The device has been characterised with a synchrotron micro-beam by mapping the X-ray beam induced current as a function of position and electrical field strength. The results provide the first proof of principle of a diamond detector device with bulk electrodes.

2. Diamond detector fabrication

A single crystal CVD diamond produced by Element Six Ltd. was used as detector material. The sample was so called electronic grade diamond with an impurity level from nitrogen below 5 ppb and a charge collection efficiency of close to 100%. The dimensions of the sample were 4.7 mm × 4.7 mm with a thickness of 500 μm.

The conductive GMCs have been fabricated following an established process [5], [6], [7], [8]. A focused laser beam is moved across the diamond plate. In the focal point the energy is

sufficient to induce a diamond to graphite phase transition. To process the samples a Nitrogen laser operating at $\lambda = 337$ has been used (MNL 100, Lasertechnik Berlin GmbH), providing single pulses of 3 ns duration with a 30 Hz repetition rate. The initial energy (150 μJ/pulse) has been lowered to 4.67 μJ/pulse using neutral density filters. The laser beam has been focused with a microscope lens providing a fluence of 5.95 J cm^{-2} and a laser spot diameter of 10 μm. The sample has been moved relative to the laser spot with a speed of 20 μm s^{-1} to create graphitic structures.

Diamond graphitisation is a process that takes few picoseconds [9]. A localised transformation of diamond into graphite induces internal strain on the surrounding lattice due to the lower density of graphite and thus expansion in volume compared to diamond. It has been shown [9], [10], [11] that a small graphitic area with negligible lattice heating or damage in the surrounding diamond lattice is created with a laser pulse duration of up to a few picoseconds. For this experiment we used a pulse duration of nanoseconds, which leads to a significant larger energy transfer resulting in strained areas where macroscopic cracks can occur when the strain exceeds the diamonds' tensile strength, and may lead to a change in the band-structure and of carrier mobilities as shown for silicon [12]. The strain formation due to the graphite–diamond phase transformation in vicinity of the GMCs has been studied using birefringence microscopy. Fig. 1(a) shows a birefringence picture of the 5 by 5 electrode matrix with a spacing of 200 μm between the columns, and in Fig. 1(b) a photograph after metallisation is shown. A high level of internal stress is visible, concentrating in the vicinity of the columns. On the right side a crack is visible which developed after the laser processing and is due to the high internal stress. The photograph of the metallisation shows that the crack intercepts the metallisation lines which lead to an inferior contact to the third and fifth bias line when counted from the top.

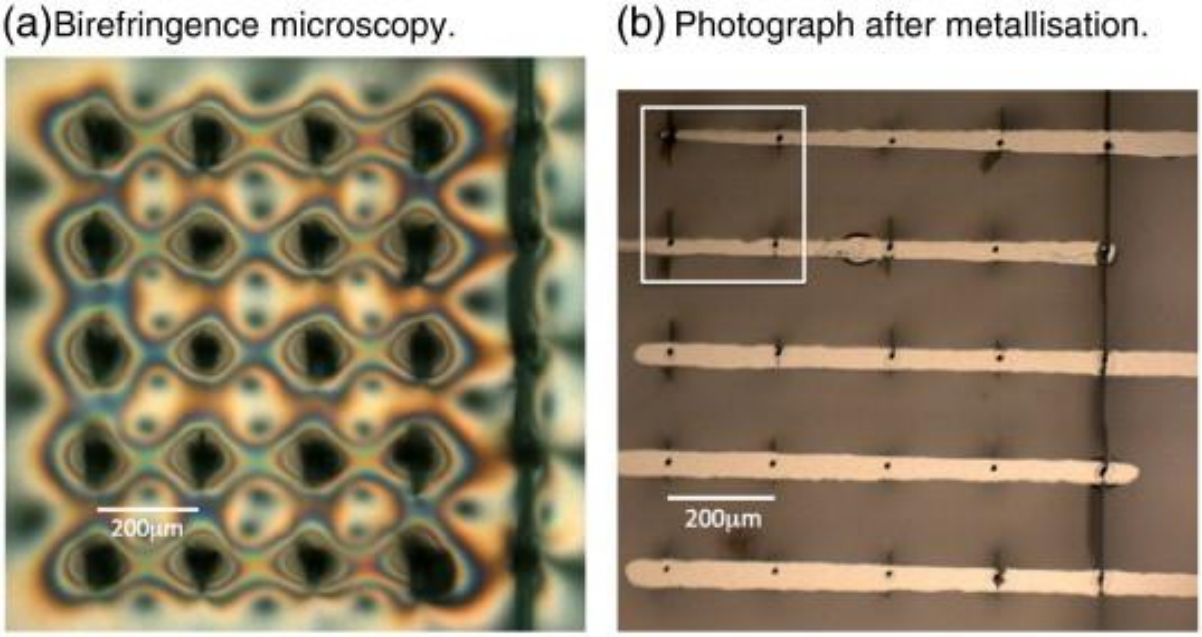

Fig. 1. The picture of a single crystal sample with an array of graphitic columns from birefringence microscopy is shown in (a), and the sample after metallisation is shown in picture (b). The white box indicates the area where measurements with the photon-micro beam have been taken.

To study the material composition of the electrode the Raman spectrum was investigated using a focal Raman microscope Witec alpha300 at a wavelength of 532 nm and a spot size of $< 1\,\mu$m and a power of 3 mW. A typical spectrum together with a SEM picture of the electrode is shown in Fig. 2. The wide bands at around 1340 cm^{-1} and 1570 cm^{-1} correspond to the D peak of micro-crystaline graphite and to the G peak of graphite [13], respectively. The Raman spectra taken on various other columns show similar spectra indicating that the columns consist of a mixture of different forms of graphite.

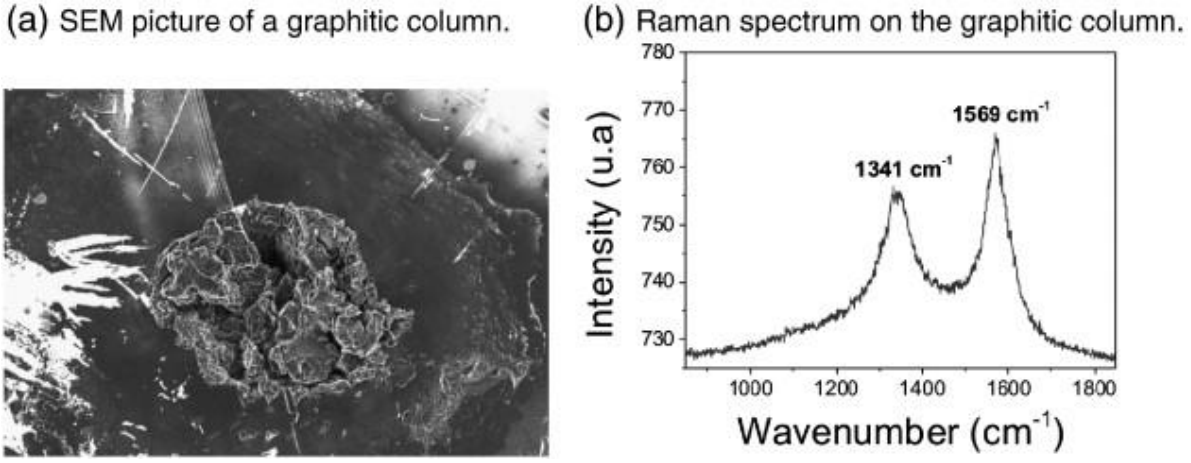

Fig. 2. SEM picture of a graphitic column (a) on which a Raman spectrum (b) was obtained.

The resistance of ten GMCs has been measured with a current–voltage measurement set-up as detailed in Fig. 3(a). The sample has been glued to a copper plate using silver paste establishing the back-side contact to the GMCs. The front-side channel end was coated with an evaporated Al layer with a thickness of 100 nm and contacted using a gold tip. Fig. 3(b) represents the current averaged over ten GMCs as a function of voltage. The GMCs exhibit an ohmic behaviour and their resistance has been determined to be 3.3 kΩ with a standard deviation of 0.2 kΩ for a channel length of 500 μm, corresponding to a resistivity of about 0.1 Ω cm. The measured resistivity is higher than for graphite powder under compression ((10^{-4}) Ω cm [14]), and slightly lower than values reported for photo-induced amorphous structures in synthetic diamond with a femto-second laser ((1) Ω cm [7]).

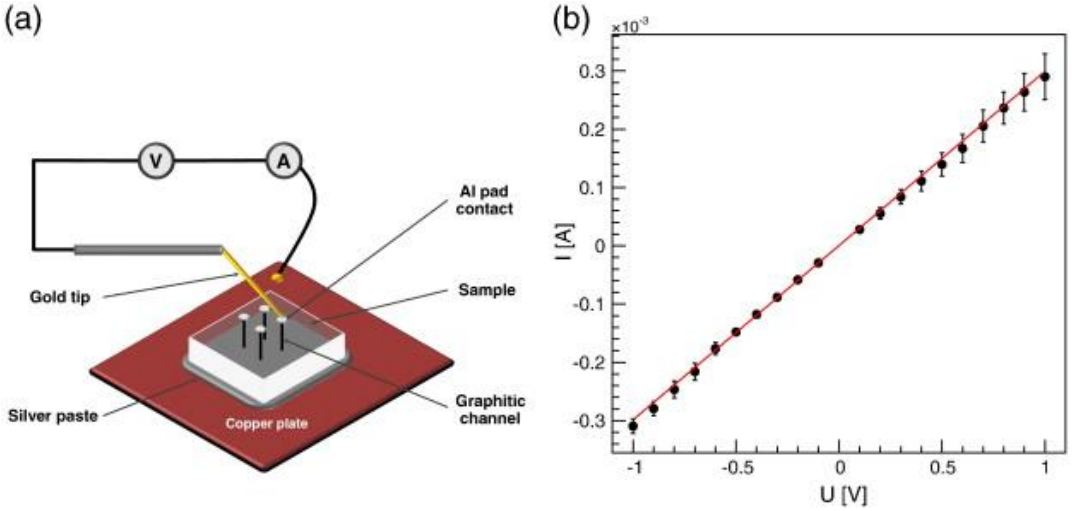

Fig. 3. Set-up to measure I–V curves (a) and average current of ten GMCs as a function of voltage with error-bars indicating the standard deviation at each measurement point. (b).

3. XBIC with a 15 keV photon micro beam

The beam-line B16 [15] at the Diamond Light Source Ltd. in Didcot was used to study the detector by X-ray beam induced current (XBIC). The beam-line was set-up to provide a monochromatic beam of photons with an energy of 15 keV. The absorption length in diamond of photons at this energy is about 4 mm, consequently the ionisation density produced by the photon beam is in good approximation uniform over the full length of the trajectory within the sample (500 μm).

Compound refractive lenses were used to obtain a focused beam. The dimensions of the beam were determined by knife-edge scans of the beam profile with a gold wire of 200 μm in diameter. The full width at half maximum was measured to be 2.1 μm in the vertical and 3.0 μm in the horizontal plane. The range of electrons in the diamond with a kinetic energy of 15 keV is about 1.7 μm [19], resulting in an effective ionisation width of the beam of less than 7 μm. The photon flux of the beam was determined with an ionisation chamber to be in the range of 10^9–10^{10} photons per second depending on the chosen absorber settings in the beam-line. The variations due to current changes in the synchrotron ring were measured to be less than 0.4%.

The samples were mounted in a metal box with aluminium foil entrance windows to shield against light and electromagnetic noise. The box was mounted on a 5-circle Huber diffractometer with an XYZ sample stage to scan the sample surface. The accuracy of the spatial translation was about 1 μm. The sample was scanned in X and Y for area scans of about 1 mm by 1 mm. Additionally, various line scans were performed for different bias voltages.

The detector response was studied by measuring the X-ray beam induced current, I, as a function of the position of the beam on the sample. A current amplifier (Keithley 428) with a rise time of 50 ms was used to measure the signal. A data acquisition system (DAQ) was recording the current measurements of the device under test, the beam position, the current of the ionisation chamber, and the ring current of the accelerator. A schematic of the diamond detector set-up in the photon-beam is shown in Fig. 4.

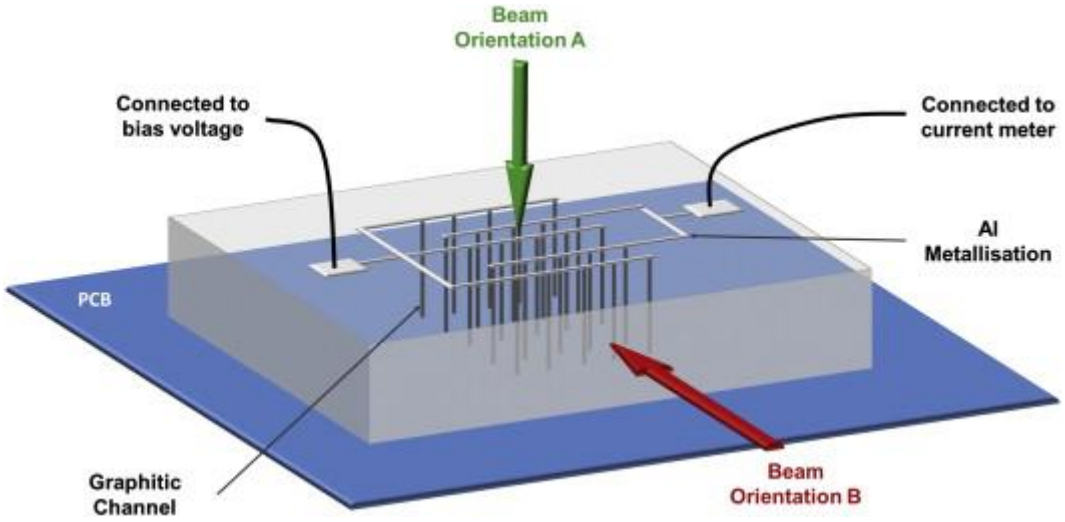

Fig. 4. Schematic of the diamond detector set-up in the photon-beam.

Line scans across two columns in beam orientation A as indicated in Fig. 4 at different bias voltages and polarities are shown in Fig. 5. The increase of signal with bias voltage is shown in Fig. 5(a). The shape of the line scan remains similar at different voltages. Clearly visible is the decrease of signal when the beam is at the centre of the column, an area where no signal creation is expected. The response is up to 300 nA and likely limited by space charge effects due to the high ionisation density. The corresponding induced current at full charge collection is estimated to be about 490 nA.

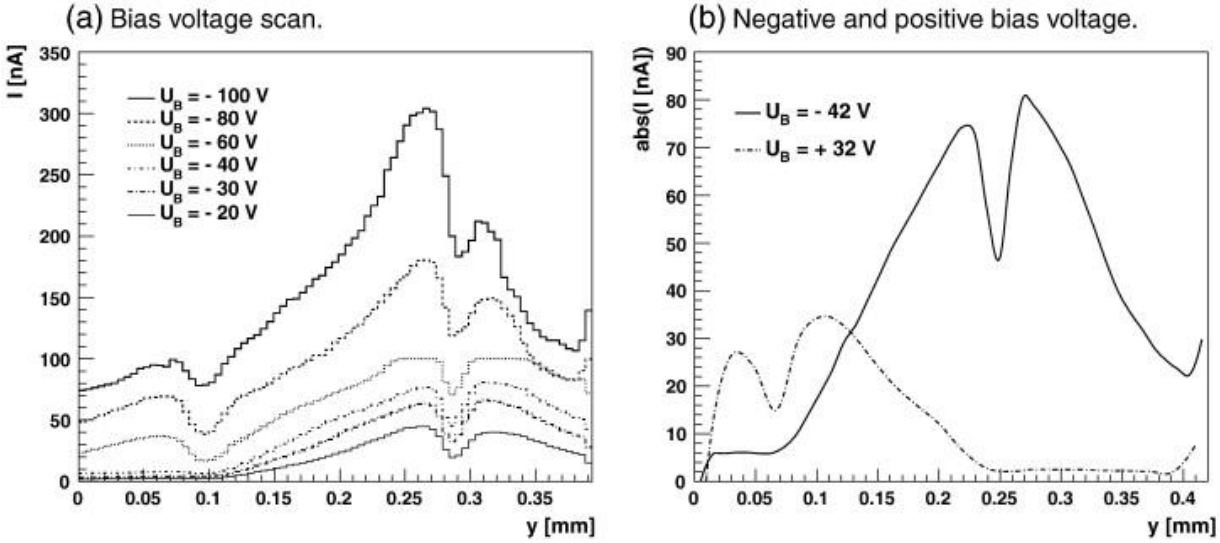

Fig. 5. Line scans across two graphitic columns at different bias voltages values (a) and polarities (b).

Scans with negative and positive polarities of the bias voltage as shown in Fig. 5(b) reveal a complementary response. The bias voltage is applied to the electrode located at $y \approx 0.3$ mm, and the current amplifier is connected to the electrode at $y \approx 0.1$ mm. The enhanced signal at the negative electrode indicates that the electron contribution dominates the signal. A scan of a four column area of about 0.4 mm by 0.4 mm is shown in Fig. 6 for positive (a) and negative (b) polarities, indicating also the position of the line scan shown in Fig. 5. The matrix of columns is clearly visible and the response exhibits a radial symmetry with the graphitic column at the centre.

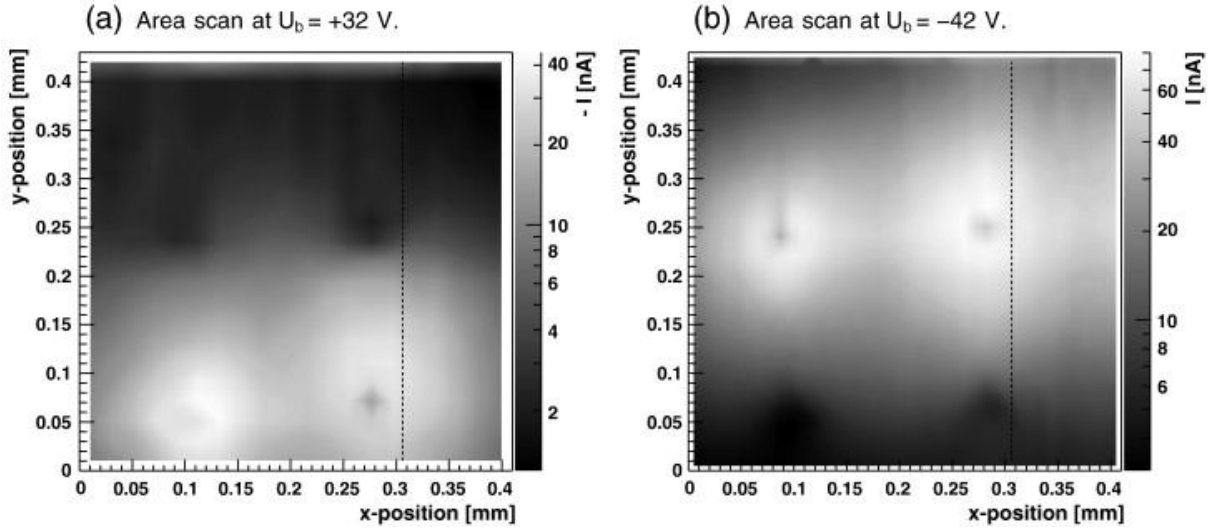

Fig. 6. Area scans around four graphitic columns at positive (a) and negative (b) bias polarities.

The dominance of the electron contribution to the signal is clearly seen also in the area scans. This asymmetry in carrier contribution has also been observed with "buried graphitic electrodes" in single crystal diamond produced by ion-beam implantation [16] and characterised with ion beam induced current. A possible explanation for this behaviour could be that the lifetime of hole carriers are much shorter than for electrons as proposed in [16]. However, direct measurements of the life-time and mobility of electrons and holes in single crystal diamond with alpha particles [17], [18] do not support this view, but show evidence for the existence of a negatively charged space-charge density showing a bias-voltage dependence. This can lead to field free region in the bulk, especially for low bias-voltages. Furthermore, the interface between the GMC and the diamond bulk may contain various defects which could act differently on electrons and holes. Further studies are being prepared to understand the charge asymmetry of the signal response with simulations.

Fig. 7 shows a scan taken perpendicular to the columns by directing the photon-beam into the side of the detector. This set-up is indicated in Fig. 4 as beam configuration B. The scan area is about 0.4 mm by 0.6 mm with a stepping size of 7 μm and again a bias of $U_b = -40$ V was applied. The data indicates that the device is active over the full length of the columns.

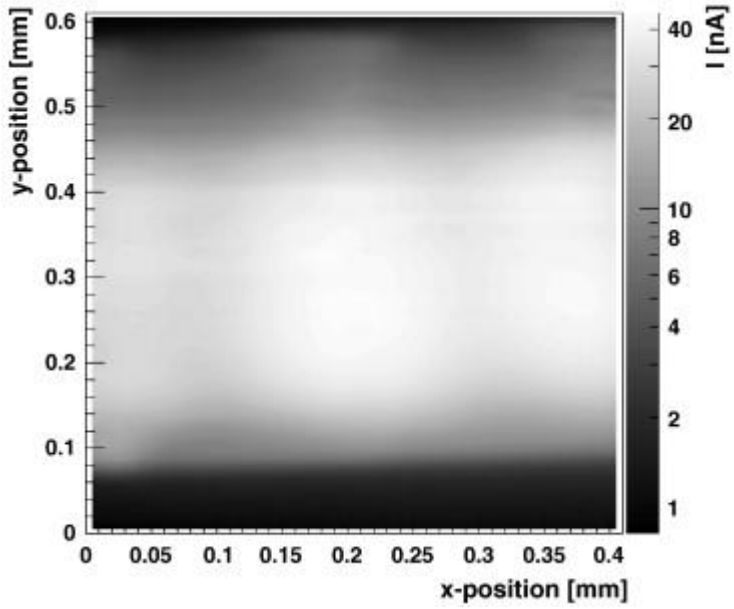

Fig. 7. Area scan of the detector edge at $U_b = +32$ V.

4. Conclusions

We described a method to produce a 3D diamond detector using graphitic columns in the bulk produced by laser graphitisation as electrodes. A prototype detector was tested with synchrotron micro-beam, and the spatial response to ionising radiation was measured. The results demonstrate for the first time the feasibility of a 3D diamond detector device.

Prime novelty statement

A single crystal CVD diamond sample has been prepared with an array of graphitic wires by laser induced graphitisation and the functionality of this "3D diamond detector" for ionising radiation has been demonstrated.

Acknowledgement

We would like to thank Dr. Kawal Sawhney and Dr. Slava Kachkanov from Diamond Light Source Ltd. for the support at the beam-line B16, Dr. José Alvarez from Laboratoire de Génie Electrique de Paris for the Raman characterisation, and Dr. Cinzia Da Via and Prof. Stephen Watts from the University of Manchester for their collaboration in requesting the joined beam-time used to obtain these results. AO would like to acknowledge support from the Royal Society.

References

[1] H. Kagan. Nucl. Instrum. Methods Phys. Res. A, 546 (2010), pp. 222-227

[2] M. Barbero, *et al.* Technical Report LHCC-RD-012 CERN-LHCC-2007-002, CERN, Geneva (2007)

[3] A. Kok, G. Anelli, C. DaVia, J. Hasi, P. Jarron, C. Kenney, J. Morse, S. Parker, J. Segal, S. Watts, E. Westbrook. Nucl. Instrum. Methods Phys. Res. A, 560 (2006), pp. 127-130

[4] A. Oh, T. Wengler, M. Ahmed, C. Da Via, S. Watts. Diamond Relat. Mater., 20 (2011), pp. 398-402

[5] S. Gloor, W. Lüthy, H.P. Weber. Diamond Relat. Mater., 8 (1999), pp. 1853-1856

[6] T.V. Kononenko, M.S. Komlenok, V.P. Pashinin, S.M. Pimenov, V.I. Konov, M. Neff, V. Romano, W. Lüthy. Diamond Relat. Mater., 8 (2009), pp. 196-199

[7] M. Shimizu, Y. Shimotsuma, M. Sakakura, T. Yuasa, H. Homma, Y. Minowa, K. Tanaka, K. Miura, K. Hirao. Opt. Express, 17 (2009), pp. 46-54

[8] S. Pimenov, I. Vlasov, A. Khomich, B. Neuenschwander, M. Muralt, V. Romano. Appl. Phys. A Mater. Sci. Process., 105 (2011), pp. 673-677

[9] V. Kononenko, T. Kononenko, S. Pimenov, M. Sinyavskii, V. Konov, F. Dausinger. Appl. Phys. A Mater. Sci. Process., 76 (2003), pp. 603-607

[10] C. Wang, K. Ho, M. Shirk, P. Molian. Phys. Rev. Lett., 85 (2000), pp. 4092-4095

[11] V. Strekalov. Appl. Phys. A Mater. Sci. Process., 80 (2005), pp. 1061-1066

[12] E. Ungersboeck, W. Gös, S. Dhar, H. Kosina, S. Selberherr. Math. Comput. Simul., 79 (2008), pp. 1071-1077

[13] J. Schwan, S. Ulrich, V. Batori, H. Ehrhardt, S.R.P. Silva. J. Appl. Phys., 80 (1996), p. 440

[14] S. Rattanaweeranon, P. Limsuwan, V. Thongpool, V. Piriyawong, P. Asanithi. Procedia Eng., 32 (2012), pp. 1100-1106

[15] K.J.S. Sawhney, I.P. Dolbnya, M.K. Tiwari, L. Alianelli, S.M. Scott, G.M. Preece, U.K. Pedersen, R.D. Walton. AIP Conf. Proc., 1234 (2010), pp. 387-390

[16] P. Olivero, J. Forneris, M. Jakšić, Ž. Pastuović, F. Picollo, N. Skukan, E. Vittone. Nucl. Instrum. Methods Phys. Res. B, 269 (2011), pp. 2340-2344

[17] H. Pernegger, S. Roe, P. Weilhammer, V. Eremin, H. Frais-Kölbl, E. Griesmayer, H. Kagan, S. Schnetzer, R. Stone, W. Trischuk, D. Twitchen, A. Whitehead. J. Appl. Phys., 97 (2005), p. 073704

[18] M. Pomorski, E. Berdermann, W. de Boer, A. Furgeri, C. Sander, J. Morse, A. Furgeri, C. Sander, J. Morse. Diamond Relat. Mater., 16 (2007), pp. 1066-1069

[19] M.J. Berger, J.H. Hubbell, S.M. Seltzer, J. Chang, J.S. Coursey, R. Sukumar, D.S. Zucker, K. Olsen. XCOM: photon cross section database (version 1.5). National Institute of Standards and Technology, Gaithersburg, MD (2010) (http://physics.nist.gov/xcom)